

Article

Room Temperature Surfactant-Free Synthesis of Gold Nanoparticles in Alkaline Ethylene Glycol

Ditte Røjkjær Rasmussen [†], Malthe Friis Nielsen [†] and Jonathan Quinson ^{*} 

Department of Biochemical and Chemical Engineering, Aarhus University, 40 Åbogade, 8200 Aarhus, Denmark

^{*} Correspondence: jquinson@bce.au.dk
[†] These authors contributed equally to this work.

Abstract: Gold nanoparticles are easily obtained by a range of room temperature processes. In particular, polyols-based syntheses performed in alkaline conditions without the need for surfactants lead to small size nanoparticles around 10 nm in diameter. While highly viscous polyols, such as glycerol, have been the most studied polyols with which to perform the reaction, the use of alternative alcohols with lower viscosity could benefit the processing of the nanoparticles. Here, we show that ethylene glycol is a suitable alternative to glycerol. Via a study comprising more than 70 experiments overall, we identified that the key parameters by which to control nanoparticle size and colloidal stability are the amount of base used and the amount of ethylene glycol. Too-high or too-low values of base and/or ethylene glycol do not lead to stable colloidal nanoparticles. An optimal Base/Gold molar ratio is around 4 and an optimal amount of ethylene glycol is around 30 v.% to obtain stable ca. 10 nm Au NPs and to develop a green room temperature surfactant-free colloidal synthesis of gold nanoparticles.

Keywords: nanoparticles; gold; synthesis; polyol; ethylene glycol; room temperature



Citation: Rasmussen, D.R.; Nielsen, M.F.; Quinson, J. Room Temperature Surfactant-Free Synthesis of Gold Nanoparticles in Alkaline Ethylene Glycol. *Chemistry* **2023**, *5*, 900–911. <https://doi.org/10.3390/chemistry5020061>

Academic Editor: Edwin Charles Constable

Received: 17 February 2023

Revised: 13 March 2023

Accepted: 11 April 2023

Published: 14 April 2023



Copyright: © 2023 by the authors. Licensee MDPI, Basel, Switzerland. This article is an open access article distributed under the terms and conditions of the Creative Commons Attribution (CC BY) license (<https://creativecommons.org/licenses/by/4.0/>).

1. Introduction

Gold (Au) nanoparticles (NPs) present unique properties relevant for applications as diverse as catalysis [1], optics [2], sensing [3], and medicine [4]. With the wide interest and potential use of Au NPs, numerous synthetic recipes have been reported. In particular, various colloidal syntheses of Au NPs have been documented [5]. In these approaches, a metal precursor, such as HAuCl_4 , is reduced to Au NPs in a solvent and in the presence of at least one reducing agent. In most cases, *additives* playing the role of size-controlling and/or shape-directing agents are also required. These additives are usually referred to under the generic wording of *stabilizers* or *capping agents*, but also *ligands* or *surfactants*. Iconic examples of colloidal syntheses include the Turkevich–Frens method performed in close-to-boiling point water with citrate as a stabilizer and reducing agent [6,7], or the Brust–Schiffrin method performed at room temperature in the presence of a strong reducing agent such as NaBH_4 and thiol-based compounds as stabilizing agents [8].

Following the increasing concerns about sustainability, and guided by the principles of *Green Chemistry*, the design of a range of alternative synthetic concepts emerged to achieve more sustainable and eco-friendly syntheses of NPs [9–11]. In particular, due to the high reduction potential of HAuCl_4 , a range of room temperature syntheses can be achieved [5]. Examples of such room temperature syntheses use bio-derived molecules such as plants, fruits, or food extracts as reducing agents and stabilizers [12,13]. Bio-organisms such as viruses or bacteria are also suitable for obtaining Au NPs [14]. Unfortunately, depending on the source of these species, different results and impacts on the Au NPs properties are expected, for instance because extracts from bio-derived sources have different properties depending on the origin of the feedstock [15]. Although such biogenic approaches are arguably *green* (obtaining plant extracts might require the generation of organic waste), they hardly address the challenges of reproducibility often observed in NP syntheses [16].

Fortunately, as an alternative, a range of syntheses are possible using simple and safe chemicals such as polyols [17,18]. For instance, the group of Prof Tremiliosi-Filho and others reported the room temperature synthesis of Au NPs using glycerol [19–21]. The reaction proceeds under alkaline conditions where alkoxides from the alcohol play the role of reducing agents [22]. While the synthesis is often performed in the presence of stabilizers such as polyvinylpyrrolidone (PVP), an additive commonly used in the synthesis of various nanomaterials [23], the same group showed that no stabilizers are required to obtain stable colloidal NPs using glycerol and water [24]. The development of surfactant-free syntheses, although it remains a general challenge, is indeed possible [25] and directly beneficial for applications such as catalysis where more active ‘unprotected’ or ‘surface clean’ NPs typically show higher catalytic activity than their counterpart prepared with surfactants [26]. Developing surfactant-free syntheses also alleviates the typically tedious, multi-steps and energy demanding removal of the surfactants [27]. Most polyols are relatively safe chemicals, such as glycerol [24]. Unfortunately, glycerol and its mixtures with water lead to highly viscous media (the viscosity of glycerol is about 1.4 Pa·s) that can be tedious to handle and process [28]. High viscosities can be detrimental to scaling up the synthesis, for instance in flow systems, or for further using the as-prepared colloids. In a range of surfactant-free syntheses based on the so called ‘polyol synthesis’ [17], ethylene glycol (EG) is preferred. EG is also a relatively green solvent [29] suitable for obtaining Pt, Ir, Ru, or Rh NPs [26,30,31].

However, obtaining surfactant-free Au NPs using EG following the recipes developed for other precious metal NPs often leads to large gold nuggets. This is attributed to the typically high concentration of metal precursors used in the polyol-EG synthesis (typically around 20 mM), the high amount of reducing agent (syntheses are often performed in 100% polyols) and the high temperature required (typically close the boiling point of the polyol) [30,32,33]. Using HAuCl₄ as a precursor, the combination of these conditions leads to the rapid formation of large Au-based materials beyond the nanoscale. Nevertheless, although EG and its mixtures with water are less viscous than solutions obtained with glycerol (the viscosity of EG is around 1.6×10^{-2} Pa·s) [34], using EG still requires a flocculation step in acid to collect the NPs before further use [35]. This suggests that stable Au NPs could be obtained using EG under the right conditions. Inspired by the results showing that glycerol is suitable for developing surfactant-free colloidal Au NPs at room temperature, and taking into account the fact that EG should be a suitable solvent for reducing HAuCl₄ and stabilizing surfactant-free NPs, here, we investigated the option to substitute glycerol with EG.

Previous reports on surfactant-free colloidal syntheses of Au NPs using glycerol focused on the influence of the amount of glycerol (typically in the range 20–100%) [24,36], the amount of base (typically in the range 1 mM up to 300 mM) [24,36], and/or the temperature (typically in the range 10–60 °C) [24]. The HAuCl₄ concentration is typically in the range 0.5–1.0 mM, which means that the Base/Au molar ratio is typically around 1–10 [36], up to 400 [24]. A relatively high amount of glycerol is often preferred, e.g., around 65 v.%, to obtain ca. 7 nm Au NPs. It has been suggested that the viscosity of glycerol was the key to stabilizing the NPs [24]. The opportunities opened by room temperature syntheses are extremely appealing considering that at too-high temperatures (above 60 °C) larger NPs are obtained and the reaction proceeds anyway within a few minutes at room temperature [24]. Room temperature syntheses are suitable for obtaining relatively small ca. 7 nm NPs, which make the use of higher temperatures relatively irrelevant in the context of developing energy-efficient syntheses. In most polyol processes, the amount of base and/or the Base/Au molar ratio control the size of the NPs [37] and, in the case of surfactant-free glycerol-based syntheses, one report focused on the use of a Base/Au molar ratio of around 200 to lead to ca. 7 nm Au NPs, using 65 v.% glycerol [24], whereas another work achieved about the same size with only a molar ratio of Base/Au of 1.3 and 20 v.% glycerol [36]. These results suggest that surfactant-free and room temperature syntheses of Au NPs could be achieved (i) substituting glycerol with EG in low(er) viscosity media, (ii) using a low

amount of reducing agent, and (iii) minimizing the amount of base. These opportunities to develop such green(er) syntheses were explored here.

2. Materials and Methods

2.1. Chemicals

All chemicals were used as received. $\text{HAuCl}_4 \cdot 3\text{H}_2\text{O}$ ($\geq 99.9\%$, Sigma Aldrich, St. Louis, MO, USA); ethylene glycol (EG, EMSURE[®] Reag. Ph Eur, Reag. USP, Supelco); $\text{LiOH} \cdot \text{H}_2\text{O}$ (ACS reagent, $\geq 98.0\%$, Sigma Aldrich); water (Milli-Q, Millipore, resistivity of $>18.2 \text{ M}\Omega \cdot \text{cm}$); HCl (puriss. ACS reagent, reag. ISO, reag. Ph. Eur. fuming, $\geq 37\%$, Sigma Aldrich); HNO_3 (puriss $\geq 65\%$, Sigma Aldrich).

2.2. Synthesis of Au NPs

The syntheses were performed following the general procedure reported elsewhere [24,36], with adjustments. Stock solutions of 50 mM HAuCl_4 in water and 50 mM LiOH in water were prepared in glassware and plasticware (polyethylene), respectively. A stock solution of 66 v.% EG in water was used (obtained by dilution of the 100% EG commercially available). As opposed to previous work on glycerol where it is not clear if and how the solution was stirred [36] or where a ‘soft shake’ was performed [24], stirring at 500 rotations per minutes was used. A magnet cleaned with *aqua regia* (prepared using a mixture of 4:1, v:v, $\text{HCl}:\text{HNO}_3$) was placed in ca. 8 mL glassware. The desired amount of water, EG, and LiOH from the stock solutions were added and the solution was magnetically stirred. Upon stirring, the desired amount of HAuCl_4 was added last at ambient temperature and in ambient light. The container was then closed with the dedicated cap. Although the reaction proceeded rapidly within few minutes and was completed in few hours, as assessed by the appearance of a red color, the solutions were left to stir for 24 h before any further characterization was performed, and the samples were subsequently stored at room temperature.

The total volume of the solutions was 3 mL and the final HAuCl_4 concentration was 0.5 mM. The volumes of water, EG, LiOH , and HAuCl_4 were therefore adjusted to investigate 10, 20, 30, 40 or 50 v.% EG and $\text{LiOH}/\text{HAuCl}_4$ molar ratios of 2.5, 3.0, 3.5, 4.0, 4.5, 5.0, 6.0, 9.0, 12.0, or 15.0, as summarized in Table 1. These relatively low values for EG contents and the amount of base were preferred to develop relatively *green* syntheses, i.e., with low amounts of alcohols and low amounts of base.

Table 1. Overview of the parametric space investigated for the synthesis of Au NPs using EG as the reducing agent. The final concentration of HAuCl_4 was 0.5 mM, the final volume 3 mL, and LiOH was used as the base.

EG v.% in Water	$\text{LiOH}/\text{HAuCl}_4$ Molar Ratio
10	2.5, 3.0, 3.5, 4.0, 4.5, 6.0, 9.0, 12.0, 15.0
20	2.5, 3.0, 3.5, 4.0, 4.5, 6.0, 9.0, 12.0, 15.0
30	2.5, 3.0, 3.5, 4.0, 4.5, 5.0, 6.0, 9.0, 12.0, 15.0
40	2.5, 3.0, 3.5, 4.0, 4.5, 5.0, 6.0, 9.0, 12.0, 15.0
50	2.5, 3.0, 3.5, 4.0, 4.5, 5.0, 6.0, 9.0, 12.0, 15.0

2.3. Characterization

2.3.1. UV-vis Spectroscopy

UV-vis spectra were acquired with a Thermo Scientific Genesys 10S UV-vis spectrophotometer with measurements performed in the range 300–800 nm. The measurements were performed on the as-prepared colloids in the liquid phase. A mixture with the same water:EG ratio as the sample was used as a baseline, without base. The as-prepared solutions were placed in dedicated UV-vis polystyrene cuvettes with a 1 cm width for absorption measurements.

Due to their pronounced surface plasmon resonance (spr) properties, Au NPs can easily yet comprehensively be characterized by UV-vis [38,39] with a relatively high throughput

method relevant to characterizing the relatively high number of samples considered in the present study (over 70 overall). Various metrics specific to Au NPs are reported in the literature and are summarized in Table 2. Au NMs show a signal in UV-vis characterization that corresponds to a size-, shape-, and solvent-dependent localized spr signal [39]. λ_{spr} is the wavelength at the spr, which corresponds to the maximum absorption peak intensity (A_{spr}) at around 520 nm. λ_{spr} values provide information on the size of spherical NPs. In a first approximation, if $525 < \lambda_{\text{spr}} < 579$ nm, the smaller λ_{spr} values indicate smaller NPs (although very small Au NPs below 3–4 nm do not show a pronounced A_{spr}) [38]. For larger NMs or aggregated NPs, the plasmon peak position shifts to higher wavelengths. The relative width at 90% of A_{spr} , $\Delta\lambda/\lambda_{\text{spr}}$, evaluates the broadness of the spr peak, and indirectly gives an indication on the broadness of the size distribution [40]. A_{spr}/A_{450} (where A_{450} is the absorbance at 450 nm) gives an indication of the size of the NPs. The equations derived from the Mie theory and the values typically used were obtained in pure water and cannot be directly used here in mixtures of water and alcohol [38,39]. A lower A_{spr}/A_{450} value corresponds to smaller NPs [38]. A_{650}/A_{spr} (where A_{650} is the absorbance at 650 nm) indicates the extent of the aggregation of the NPs [41,42]. Higher A_{650}/A_{spr} ratios indicate more aggregated NPs (note that this is only true if the NPs are characterized by a well-defined plasmon resonance peak). A_{380}/A_{800} (where A_{380} is the absorbance at 380 nm and A_{800} is the absorbance at 800 nm) indicates the stability of the colloids. The most stable colloids display a higher ratio [43]. **The relative intensity measured at 400 nm** (A_{400}) indicates the relative amount of Au⁰ in the sample, and so provides an estimation of the relative yields of the syntheses [39].

Table 2. Overview of the Au NPs properties retrieved from UV-vis spectroscopy.

Values	Property	Indicates
λ_{spr}	spr	Size (lower values correspond to smaller sizes)
$\Delta\lambda/\lambda_{\text{spr}}$	Broadness of the peak at 90% of A_{spr}	Size distribution (higher values correspond to larger size distributions)
A_{spr}/A_{450}	Ratio of absorbances at λ_{spr} and 450 nm	Size (lower values correspond to smaller sizes)
A_{650}/A_{spr}	Ratio of absorbances at 650 nm and λ_{spr}	Aggregation (lower values correspond to less aggregated samples)
A_{380}/A_{800}	Ratio of absorbances at 380 and 800 nm	Stability (higher values correspond to more stable colloids)
A_{400}	Absorbance at 400 nm	Relative yields

2.3.2. Scanning Transmission Electron Microscopy (STEM)

STEM micrographs were obtained on an FEI Talos F200X operated at 200 kV equipped with a High-Angle Annular Dark-Field (HAADF) detector. The as-prepared colloidal dispersions were dopped on Nickel TEM grids (Quantifoil) after dilution in ethanol. The solvent was left to evaporate and so the measurements were performed on dried NPs. The size of the NPs was retrieved from the analysis of over 500 NPs with the software ImageJ.

3. Results

The objective of this study was to investigate the possibility of using EG as a reducing agent in the synthesis of surfactant-free colloidal NPs and to investigate how different experimental parameters impact the size, shape, and stability of the Au NPs. Due to the relatively large number of experiments performed (over 70 overall), not all samples could be analyzed by all possible techniques and UV-vis was preferred to assess the resulting properties, as detailed in the *Materials and Methods* section. During the screening, focus was on the influence of the Base/ HAuCl_4 molar ratio (also equivalent to the Base/Au molar ratio) and the amount of EG in the solvent. To develop *green* syntheses, a driving force in the performed parametric study was to investigate how little of these chemicals is needed

to obtain stable surfactant-free Au NPs. To maximize the use of Au, an incentive was to develop small size NPs and the development of an optimized synthesis was guided by the values retrieved from UV-vis characterization (e.g., to achieve lower λ_{spr} values indicative of smaller sizes).

3.1. Ethylene Glycol as Reducing Agent for Au NP Synthesis

Using EG as a reducing agent leads to Au NPs with a well-defined spr. Upon adding HAuCl_4 to an alkaline mixture of water and EG, the solution turns dark, then grey, then purple, and finally red as illustrated in Figure 1a. This color change takes from between a few minutes to ca. 1 h to be observed. This color is typical of Au NPs and confirms that the reactions have proceeded using EG, as further assessed by the characteristic UV-vis spectrum obtained and reported in Figure 1b, with a pronounced spr peak at around 520 nm. The formation of Au NPs is further confirmed by STEM data reported in Figure 1c. An analysis of the data retrieved confirmed that ca. 10 nm NPs are obtained.

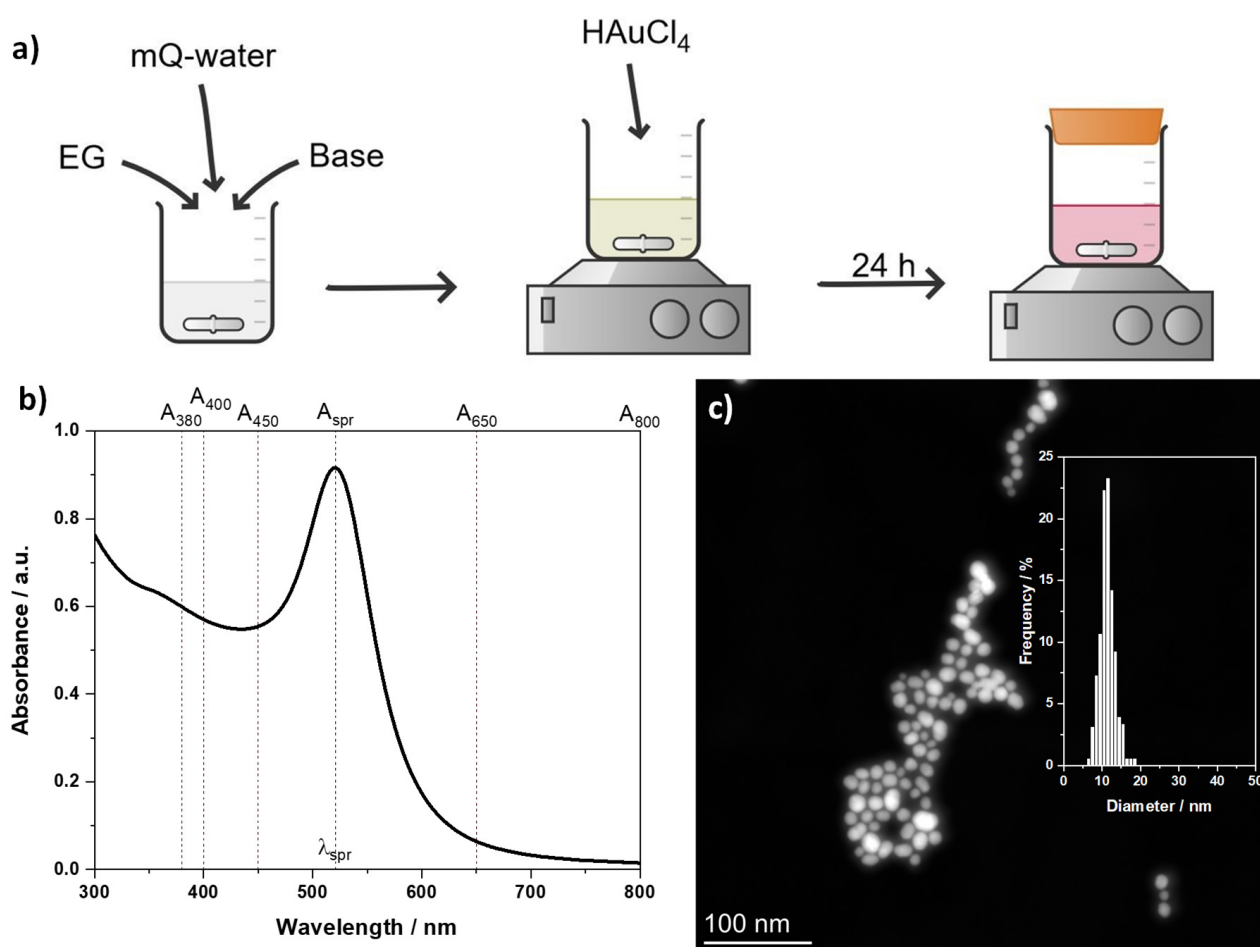


Figure 1. (a) Schematic of the reaction, (b) example of UV-vis spectrum and relevant features, and (c) examples of STEM micrographs with size distribution for Au NPs in the inset, obtained using 40 v.% EG and a LiOH/Au molar ratio of 4. The concentration of HAuCl_4 was 0.5 mM.

3.2. Influence of the Base/ HAuCl_4 Ratio and EG Content

To investigate the effect of different variables, a range of experiments were performed for which the experimental conditions are summarized in Table 1. The results obtained are summarized in Figure 2, as well as in Figures S1–S3 and Table S1 in the Supplementary Materials.

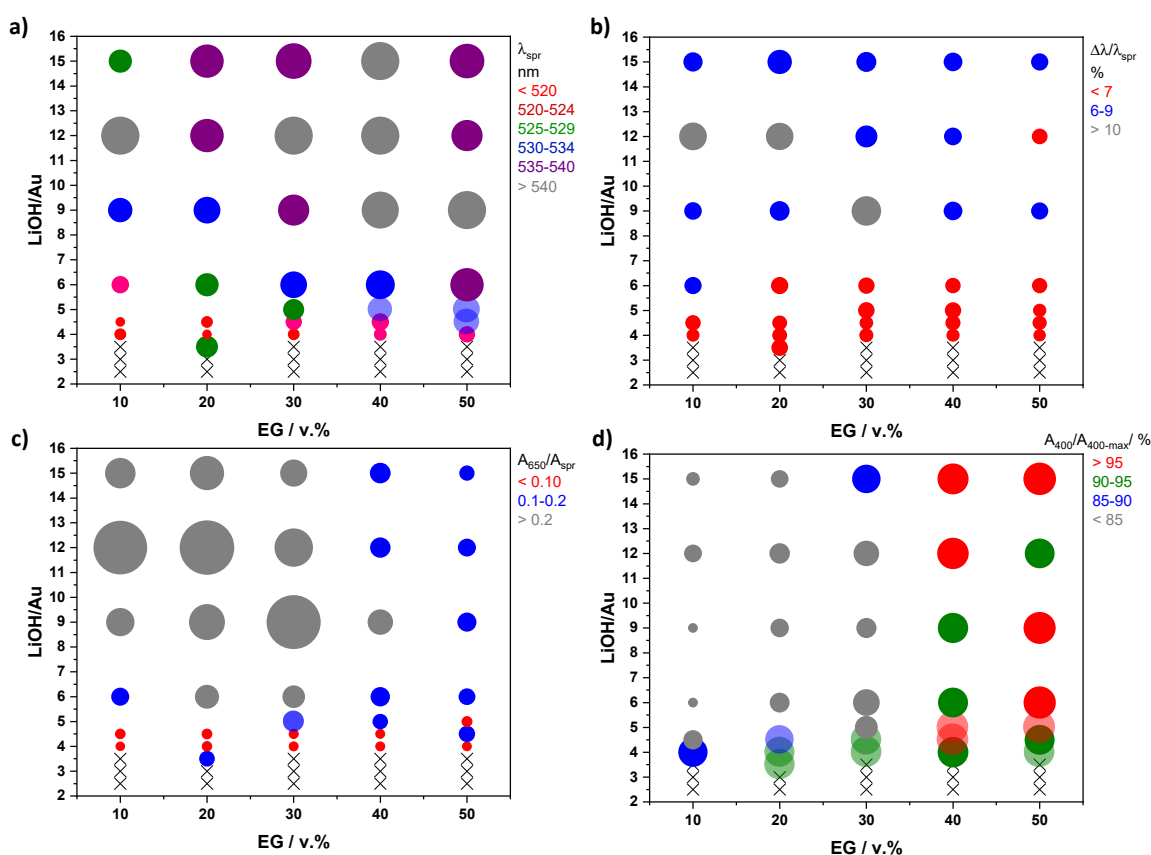


Figure 2. (a) λ_{spr} , (b) $\Delta\lambda/\lambda_{\text{spr}}$, (c) A_{650}/A_{spr} , and (d) $A_{400}/A_{400-\text{max}}$ values for samples prepared under different synthetic conditions. The size of the data points corresponding to a given v.% of EG and LiOH/HAuCl₄ molar ratio is proportional to the (a) λ_{spr} , (b) $\Delta\lambda/\lambda_{\text{spr}}$, (c) A_{650}/A_{spr} , and (d) $A_{400}/A_{400-\text{max}}$ values. $A_{400-\text{max}}$ corresponds to the maximum value of A_{400} for the dataset. To guide the readers, the desirable data point corresponding to small NP sizes, narrow size distribution, high stability, and higher relative yield are represented in red. The concentration of HAuCl₄ was 0.5 mM. An X indicates that no stable colloids were obtained. The related values are given in Table S1.

4. Discussion

4.1. Trends and Optimal Synthesis Conditions

From the performed parametric study, it is established that EG is a suitable reducing agent with which to prepare surfactant-free Au NPs, see Figure 1. The size range around 10 nm is equivalent to what has been reported using glycerol [24,36]. EG is less viscous than glycerol and this presents an advantage for the later use and upscaling of the synthesis.

From the results presented in Figure 2, we first used λ_{spr} and $\Delta\lambda/\lambda_{\text{spr}}$ values as indicators of the NP size and size distribution, respectively. In Figure 2a, lower λ_{spr} values are associated with smaller size NPs (alternatively, the $\lambda_{\text{spr}}/A_{450}$ values provided in Figure S1a can also be considered, where lower values are associated with smaller NPs). In Figure 2b, lower $\Delta\lambda/\lambda_{\text{spr}}$ values are associated with more monodispersed NPs. λ_{spr} values are around 520 nm and as low as 517 nm, and $\Delta\lambda/\lambda_{\text{spr}}$ are typically around 6%. From the parametric study performed, it is concluded that, overall, (i) the NP size increases as the EG content increases and (ii) at too-low or too-high base contents, NPs are not formed (too-low base content) or larger NPs are formed (too-high base content).

The effect of changing the EG contents is less pronounced than the effect of changing the amount of base. This can be explained by the fact that alkoxides formed from EG are expected to play the role of reducing agent [22]. Therefore, at too-high EG content, too much reducing agent likely leads to the overgrowth of the Au NPs. At a too-low base amount, there is not enough reducing agent formed (regardless of the amount of EG present) and at a too-high base amount, too much reducing agent is formed. Another explanation can

be added to the previous to account for the observation reported. HAuCl_4 is more easily reduced in its acid form than in its basic form [7,24]. In too-alkaline conditions (higher Base/Au molar ratios), it could be that the pathway for the reduction of the precursor is not favored and is therefore slower. Assuming that the classical nucleation theory applies [44], these conditions lead to the formation of a few seeds that (over)grow with time, leading to NPs with broader features in UV-vis and higher λ_{spr} values. Lower λ_{spr} values and more monodispersed samples were also observed using a lower amount of glycerol and a relatively low amount of base [36]. In a similar way, here, when higher amounts of base were used, smaller NPs were obtained at higher glycerol contents [24].

A worst-case scenario is then a combination of high EG content and a high concentration of base. A best-case scenario seems to use a Base/Au molar ratio of around 4. This is in agreement with previous work using ethanol as a reducing agent [45,46]. Considering a Base/Au molar ratio of around 4, the comparison of the different $\lambda_{\text{spr}}/A_{450}$ provided in Figure S1a suggests that slightly smaller NPs are obtained at lower EG contents.

To discuss the aggregation and stability of the NPs, A_{650}/A_{spr} values are first considered, where lower values indicate less agglomerated and more stable NPs in Figure 2c. The lowest values are also obtained for a Base/Au molar ratio of around 4. It is also observed that higher EG contents also lead to relatively stable Au NPs regardless of the base content, which is attributed to the higher viscosity of the solutions containing a high amount of EG. However, considering the A_{380}/A_{800} values provided in Figure S1b, it is observed that higher EG contents actually lead to less stable Au NPs than lower contents. It is therefore concluded that an optimal amount of EG must be not too high nor too low and therefore around 30 v.%.

Regarding the relative yield of the Au NPs synthesis, this question is more challenging to address since the UV-vis spectra are influenced by the properties of the surrounding media, so comparing data obtained in media containing different v.% of EG and/or base can be misleading. This comparison is nevertheless proposed in Figure 2d, where the relative yields are estimated using A_{400} as a proxy. The highest relative yields are obtained for a Base/Au molar ratio of around 4. It is also observed that higher EG contents lead to higher yields.

Taking into account all these observations, it is concluded that the desired combination of small size and monodispersed surfactant-free NPs obtained with relatively high yield and with promising stability are obtained with a Base/Au molar ratio of 4 for EG content of around 30 v.%. It is also concluded that, overall, changing the Base/Au molar ratio has a stronger effect on size, size distribution, stability, and yield than changing the EG content.

4.2. Reproducibility

Reproducibility in NPs synthesis is a general challenge [16,47]. To the best of our knowledge, this aspect of room temperature surfactant-free syntheses of Au NPs has not been discussed in detail in previous work using glycerol [24,36], although triplicates are mentioned in [36]. Using a Base/Au molar ratio of 4, we assessed the reproducibility of the synthesis by performing the same experiments three times with different EG contents, for which the results are reported in Figure 3. The trend previously discussed is still observed. At a given Base/Au molar ratio of 4, the λ_{spr} values are relatively independent of the EG content, with a trend of observing slightly larger λ_{spr} values as the EG content increases, see Figure 3a. Considering the $\lambda_{\text{spr}}/A_{450}$ values, it is confirmed that smaller NPs (i.e., lower $\lambda_{\text{spr}}/A_{450}$ values) tend to form at lower EG contents, see Figure S2a. The reproducibility of the values of $\Delta\lambda/\lambda_{\text{spr}}$ is the best for 30 v.% EG, see Figure 3b. The stability of the Au NPs is about the same for all EG contents considering the A_{650}/A_{spr} values in Figure 3c or the A_{380}/A_{800} values reported in Figure S2b. However, the results obtained with EG contents lower than 30 v.% and, in particular, 20 v.%, show less reproducibility (higher standard deviation for the parameters considered here). Finally, it is confirmed that higher viscosity media lead to higher apparent relative yields, see Figure 3d.

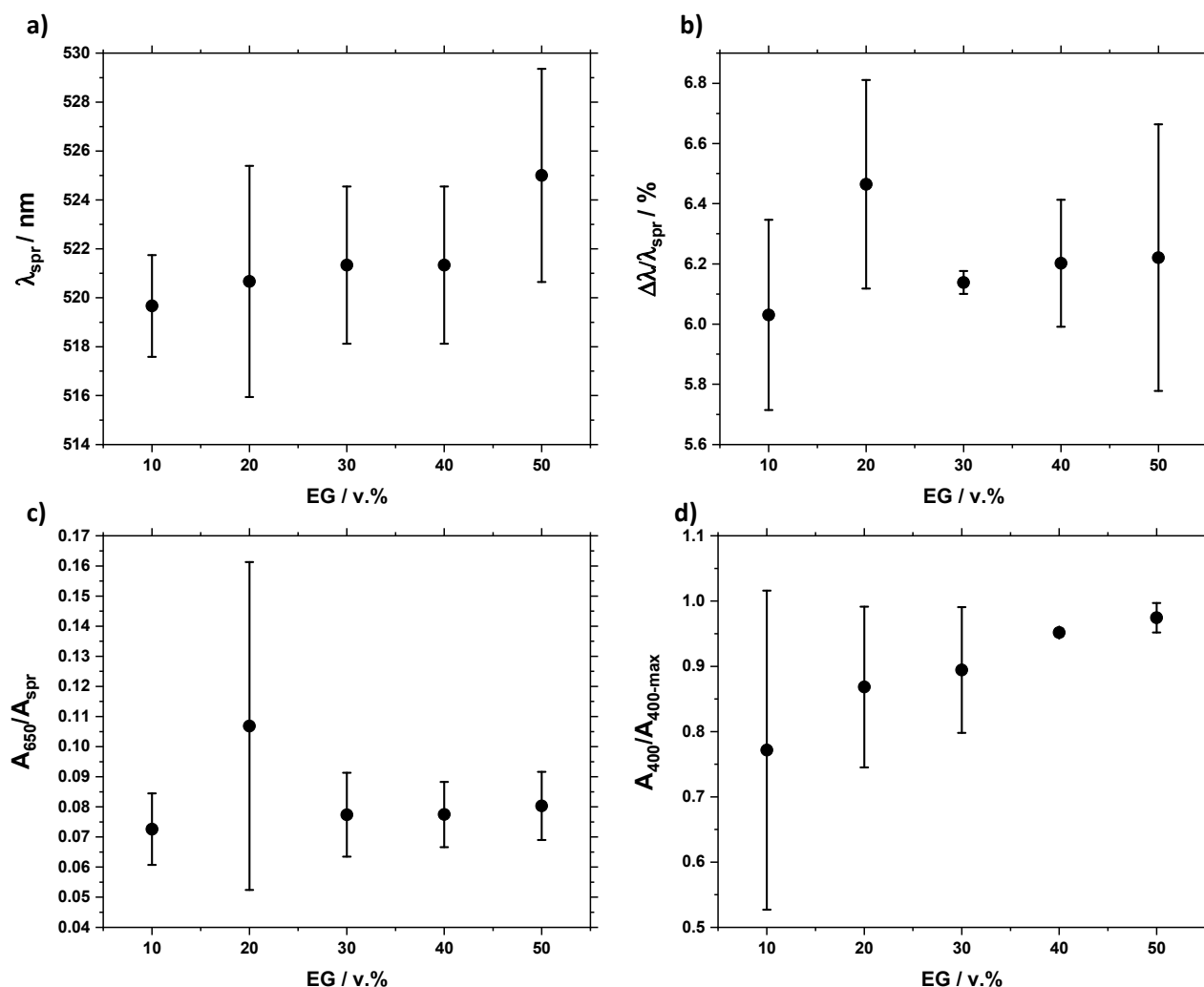


Figure 3. (a) λ_{spr} , (b) $\Delta\lambda / \lambda_{\text{spr}}$, (c) A_{650} / A_{spr} and (d) $A_{400} / A_{400-\text{max}}$ values and standard deviations for three different experiments, for samples prepared for different v.% of EG as indicated and a LiOH/HAuCl₄ ratio of 4. The concentration of HAuCl₄ was 0.5 mM.

In light of these results, to develop a *green* synthesis, minimizing the amount of chemicals required and yet achieving control over small size NPs with a reasonable yield in a reproducible way, an EG content of 30–40 v.% seems recommendable. This is lower than, for instance, the amounts of glycerol typically considered in previous investigations [24,36].

4.3. Long Term Stability

A final important aspect of the Au NPs is their stability over time, especially considering here that no surfactants were used. Stability can be improved by storing the samples in the fridge, as it was reported for glycerol-based syntheses [24]. However, we here assessed the relatively stability of different samples stored in the dark but at room temperature to assess a ‘worst-case’ scenario. Using the example of Au NPs synthesized with a Base/Au molar ratio of 4 and different EG contents, it is observed that, while the NPs show good stability for ca. a week (7 days), more pronounced changes are observed for longer periods of storage, see Figure 4 as well as Figure S3. The λ_{spr} , $\Delta\lambda / \lambda_{\text{spr}}$, A_{650} / A_{spr} , and relative yield values are rather stable for 7 days of storage in the dark and at room temperature, as well as A_{spr} / A_{450} and A_{380} / A_{800} values. After 14 days of storage, however, the UV-vis characterization suggests that NPs grow (higher λ_{spr} , $\Delta\lambda / \lambda_{\text{spr}}$ and A_{spr} / A_{450} values) and are less stable (higher A_{650} / A_{spr} values and lower A_{380} / A_{800} values). The more constant values indicative of more stable Au NP colloidal dispersions are obtained when 30 v.% EG

is used. These results further stress that a fine balance of not only the base concentration but also the amount of EG must be controlled to achieve stable Au NPs.

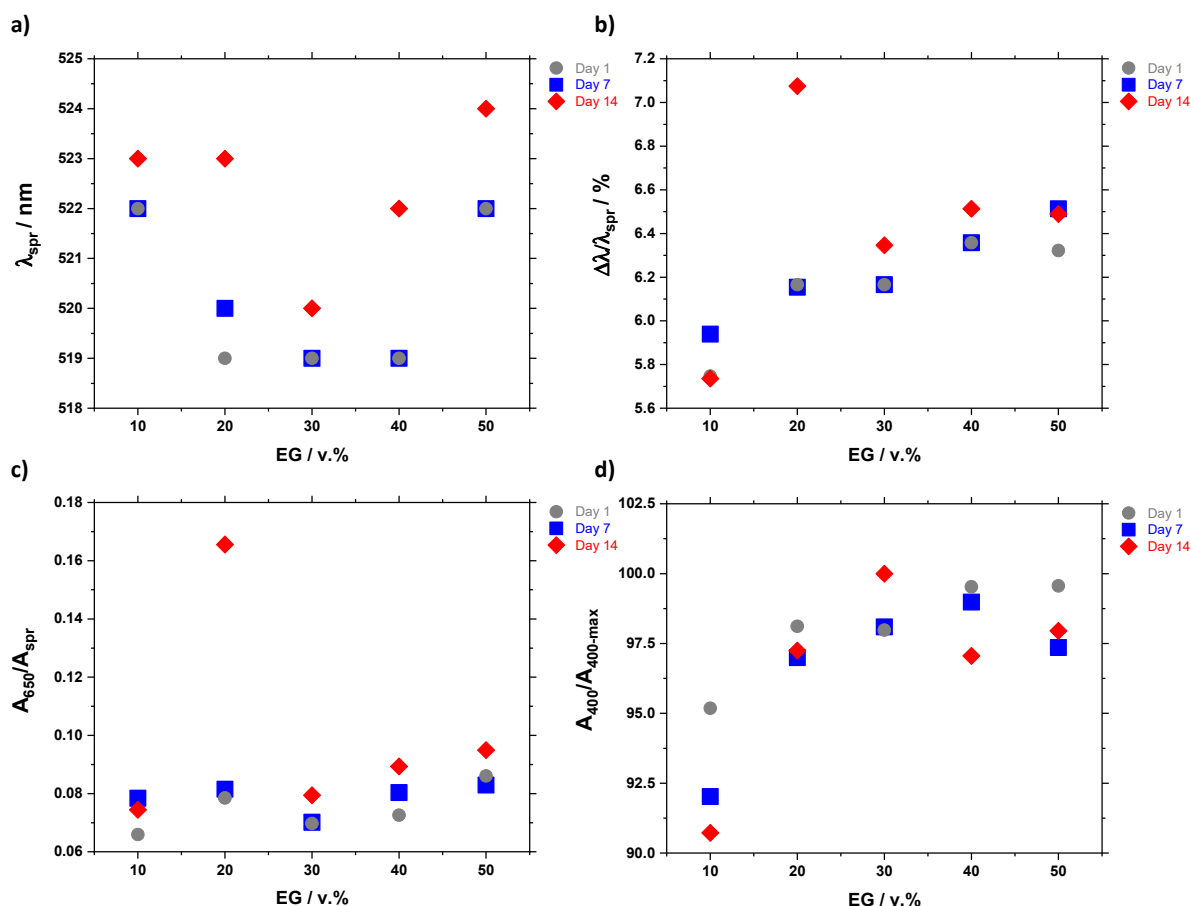


Figure 4. (a) λ_{spr} , (b) $\Delta\lambda / \lambda_{\text{spr}}$, (c) A_{650} / A_{spr} and (d) $A_{400} / A_{400-\text{max}}$ values for samples prepared for different v.% of EG as indicated and an LiOH/HAuCl₄ ratio of 4. The concentration of HAuCl₄ was 0.5 mM. The UV-vis characterization was performed 1, 7, or 14 days after synthesis, as indicated.

The relatively low values of 30 v.% EG identified in this study are in contrast with results obtained with glycerol, where an equal or higher v.% of glycerol is typically preferred to lead to stable colloids [24]. This difference can be attributed to the different viscosities of the EG and glycerol, where the more viscous glycerol might prevent further reaction of the Au NPs.

5. Conclusions

We here showed that EG is a suitable reducing agent with which to develop surfactant-free colloidal syntheses of Au NPs, ca. 10 nm in size. An optimal synthesis to minimize the Au NP size, dispersity, stability, and relative yield was performed with a relatively low LiOH/Au molar ratio of ca. 4 and a relatively low EG content of ca. 30 v.%. These results show that substituting glycerol with EG can lead to several benefits, not only using a less viscous solvent but potentially fewer chemicals (less base and less alcohol). It is also shown that, despite the absence of surfactants, the Au NPs are relatively stable over several days of storage.

There is certainly room to achieve finer size control to further develop and exploit the *green* features of the approach proposed here. For instance, we preferred LiOH as a base rather than the NaOH more commonly used for similar syntheses [24,36,46]. The assumption driving this choice was that LiOH will lead to a stronger interaction with the metal surface and will lead to more stable NPs [48,49], although LiOH is more expensive

and harmful to the environment than NaOH. Given the results discussed here, the viscosity of EG does not seem to be a major factor in the stabilization of the Au NPs that can be obtained at a relatively low EG content of 30 v.%. It could also be relevant to explore the potential of alcohol contents lower than 10 v.% for a finer size control, although lower relative yields are expected. It will also be valuable in the future to assess the effect(s) of NaOH for a deeper understanding of possible cations effect(s) in the stabilization of surfactant-free Au NPs in non-/less- viscous solvents [48], but also to develop even greener and more cost-effective room temperature and surfactant-free syntheses of Au NPs.

Supplementary Materials: The following supporting information can be downloaded at: <https://www.mdpi.com/article/10.3390/chemistry5020061/s1>, Figure S1: $\lambda_{\text{spr}}/A_{450}$ and λ_{380}/A_{800} values for the parametric study; Figure S2: $\lambda_{\text{spr}}/A_{450}$ and λ_{380}/A_{800} values for replicated experiments; Figure S3: $\lambda_{\text{spr}}/A_{450}$ and λ_{380}/A_{800} values for time studies; Table S1: Parameters retrieved from UV-vis analysis for all samples.

Author Contributions: Conceptualization, J.Q.; methodology, J.Q.; formal analysis, D.R.R. and M.F.N.; investigation, D.R.R. and M.F.N.; resources, J.Q.; data curation, D.R.R. and J.Q.; writing—original draft preparation, J.Q.; writing—review and editing, J.Q.; visualization, J.Q., D.R.R. and M.F.N.; supervision, J.Q.; project administration, J.Q.; funding acquisition, J.Q. All authors have read and agreed to the published version of the manuscript.

Funding: This research was funded by Aarhus University Research Foundation, grant number AUFF-E-2022-9-40. The APC were alleviated.

Data Availability Statement: All data are available upon request and/or available in the Supplementary Materials.

Acknowledgments: We would like to thank Espen D. Bøjesen, iNano, Aarhus University, Denmark, for training and facilitating access to the Talos F200X equipment.

Conflicts of Interest: The authors declare no conflict of interest. The funders had no role in the design of the study; in the collection, analyses, or interpretation of data; in the writing of the manuscript; or in the decision to publish the results.

References

1. Alshammari, A.S. Heterogeneous Gold Catalysis: From Discovery to Applications. *Catalysts* **2019**, *9*, 402. [CrossRef]
2. Amendola, V.; Pilot, R.; Frascioni, M.; Marago, O.M.; Iati, M.A. Surface plasmon resonance in gold nanoparticles: A review. *J. Condens. Matter Phys.* **2017**, *29*, 203002. [CrossRef] [PubMed]
3. Zeng, S.W.; Yong, K.T.; Roy, I.; Dinh, X.Q.; Yu, X.; Luan, F. A Review on Functionalized Gold Nanoparticles for Biosensing Applications. *Plasmonics* **2011**, *6*, 491–506. [CrossRef]
4. Maccora, D.; Dini, V.; Battocchio, C.; Fratoddi, I.; Cartoni, A.; Rotili, D.; Castagnola, M.; Faccini, R.; Bruno, I.; Scotognella, T.; et al. Gold Nanoparticles and Nanorods in Nuclear Medicine: A Mini Review. *Appl. Sci.* **2019**, *9*, 3232. [CrossRef]
5. De Souza, C.D.; Nogueira, B.R.; Rostelato, M. Review of the methodologies used in the synthesis gold nanoparticles by chemical reduction. *J. Alloys Compd.* **2019**, *798*, 714–740. [CrossRef]
6. Turkevich, J.; Stevenson, P.C.; Hillier, J. A study of the nucleation and growth processes in the synthesis of colloidal gold. *Discuss. Faraday Soc.* **1951**, *11*, 55–75. [CrossRef]
7. Wüthrich, M.; Birnbaum, A.; Witte, S.; Sztucki, M.; Vainio, U.; Pinna, N.; Rademann, K.; Emmerling, F.; Kraehnert, R.; Polte, J. Turkevich in New Robes: Key Questions Answered for the Most Common Gold Nanoparticle Synthesis. *ACS Nano* **2015**, *9*, 7052–7071. [CrossRef]
8. Brust, M.; Walker, M.; Bethell, D.; Schiffrin, D.J.; Whyman, R. Synthesis of thiol-derivatized gold nanoparticles in a 2-phase liquid-liquid system. *J. Chem. Soc. Chem. Commun.* **1994**, *7*, 801–802. [CrossRef]
9. Duan, H.H.; Wang, D.S.; Li, Y.D. Green chemistry for nanoparticle synthesis. *Chem. Soc. Rev.* **2015**, *44*, 5778–5792. [CrossRef]
10. Gilbertson, L.M.; Zimmerman, J.B.; Plata, D.L.; Hutchison, J.E.; Anastas, P.T. Designing nanomaterials to maximize performance and minimize undesirable implications guided by the Principles of Green Chemistry. *Chem. Soc. Rev.* **2015**, *44*, 5758–5777. [CrossRef]
11. Hutchison, J.E. The Road to Sustainable Nanotechnology: Challenges, Progress and Opportunities. *ACS Sustain. Chem. Eng.* **2016**, *4*, 5907–5914. [CrossRef]
12. Akintelu, S.A.; Olugbeko, S.C.; Folorunso, A.S. A review on synthesis, optimization, characterization and antibacterial application of gold nanoparticles synthesized from plants. *Int. Nano Lett.* **2020**, *10*, 237–248. [CrossRef]

13. Khan, T.; Ullah, N.; Khan, M.A.; Mashwani, Z.U.R.; Nadhman, A. Plant-based gold nanoparticles; a comprehensive review of the decade-long research on synthesis, mechanistic aspects and diverse applications. *Adv. Colloid Interface Sci.* **2019**, *272*, 102017. [[CrossRef](#)] [[PubMed](#)]
14. Ahmed, S.; Annu, Ikram, S.; Yudha, S.S. Biosynthesis of gold nanoparticles: A green approach. *J. Photochem. Photobiol. B Biol.* **2016**, *161*, 141–153. [[CrossRef](#)]
15. Dauthal, P.; Mukhopadhyay, M. Noble Metal Nanoparticles: Plant-Mediated Synthesis, Mechanistic Aspects of Synthesis, and Applications. *Ind. Eng. Chem. Res.* **2016**, *55*, 9557–9577. [[CrossRef](#)]
16. Liz-Marzan, L.M.; Kagan, C.R.; Millstone, J.E. Reproducibility in Nanocrystal Synthesis? Watch Out for Impurities! *ACS Nano* **2020**, *14*, 6359–6361. [[CrossRef](#)]
17. Fievet, F.; Ammar-Merah, S.; Brayner, R.; Chau, F.; Giraud, M.; Mammeri, F.; Peron, J.; Piquemal, J.Y.; Sicard, L.; Viau, G. The polyol process: A unique method for easy access to metal nanoparticles with tailored sizes, shapes and compositions. *Chem. Soc. Rev.* **2018**, *47*, 5187–5233. [[CrossRef](#)]
18. Chahdoura, F.; Favier, I.; Gomez, M. Glycerol as Suitable Solvent for the Synthesis of Metallic Species and Catalysis. *Chem. Eur. J.* **2014**, *20*, 10884–10893. [[CrossRef](#)]
19. Garcia, A.G.; Lopes, P.P.; Gomes, J.F.; Pires, C.; Ferreira, E.B.; Lucena, R.G.M.; Gasparotto, L.H.S.; Tremiliosi-Filho, G. Eco-friendly synthesis of bimetallic AuAg nanoparticles. *New J. Chem.* **2014**, *38*, 2865–2873. [[CrossRef](#)]
20. Parveen, R.; Tremiliosi, G. A step ahead towards the green synthesis of monodisperse gold nanoparticles: The use of crude glycerol as a greener and low-cost reducing agent. *RSC Adv.* **2016**, *6*, 95210–95219. [[CrossRef](#)]
21. Gasparotto, L.H.S.; Garcia, A.C.; Gomes, J.F.; Tremiliosi-Filho, G. Electrocatalytic performance of environmentally friendly synthesized gold nanoparticles towards the borohydride electro-oxidation reaction. *J. Power Sources* **2012**, *218*, 73–78. [[CrossRef](#)]
22. Gomes, J.F.; Garcia, A.C.; Ferreira, E.B.; Pires, C.; Oliveira, V.L.; Tremiliosi-Filho, G.; Gasparotto, L.H.S. New insights into the formation mechanism of Ag, Au and AgAu nanoparticles in aqueous alkaline media: Alkoxides from alcohols, aldehydes and ketones as universal reducing agents. *Phys. Chem. Chem. Phys.* **2015**, *17*, 21683–21693. [[CrossRef](#)] [[PubMed](#)]
23. Koczkur, K.M.; Mourdikoudis, S.; Polavarapu, L.; Skrabalak, S.E. Polyvinylpyrrolidone (PVP) in nanoparticle synthesis. *Dalton Trans.* **2015**, *44*, 17883–17905. [[CrossRef](#)]
24. Parveen, R.; Ullah, S.; Sgarbi, R.; Tremiliosi, G. One-pot ligand-free synthesis of gold nanoparticles: The role of glycerol as reducing-cum-stabilizing agent. *Colloids Surf. A Physicochem. Eng. Asp.* **2019**, *565*, 162–171. [[CrossRef](#)]
25. Quinson, J. Surfactant-free precious metal colloidal nanoparticles for catalysis. *Front. Nanotechnol.* **2021**, *3*, 770281. [[CrossRef](#)]
26. Arminio Ravelo, J.A.; Quinson, J.; Pedersen, M.A.; Kirkensgaard, J.J.K.; Arenz, M.; Escudero Escribano, M. Synthesis of iridium nanocatalysts for water oxidation in acid: Effect of the surfactant. *ChemCatChem* **2020**, *12*, 1282–1287. [[CrossRef](#)]
27. Niu, Z.Q.; Li, Y.D. Removal and Utilization of Capping Agents in Nanocatalysis. *Chem. Mater.* **2014**, *26*, 72–83. [[CrossRef](#)]
28. Ferreira, A.G.M.; Egas, A.P.V.; Fonseca, I.M.A.; Costa, A.C.; Abreu, D.C.; Lobo, L.Q. The viscosity of glycerol. *J. Chem. Thermodyn.* **2017**, *113*, 162–182. [[CrossRef](#)]
29. Prat, D.; Wells, A.; Hayler, J.; Sneddon, H.; McElroy, C.R.; Abou-Shehadeh, S.; Dunn, P.J. CHEM21 selection guide of classical- and less classical-solvents. *Green Chem.* **2016**, *18*, 288–296. [[CrossRef](#)]
30. Wang, Y.; Ren, J.W.; Deng, K.; Gui, L.L.; Tang, Y.Q. Preparation of tractable platinum, rhodium, and ruthenium nanoclusters with small particle size in organic media. *Chem. Mater.* **2000**, *12*, 1622–1627. [[CrossRef](#)]
31. Bonet, F.; Delmas, V.; Grugeon, S.; Urbina, R.H.; Silvert, P.Y.; Tekaiia-Elhssissen, K. Synthesis of monodisperse Au, Pt, Pd, Ru and Ir nanoparticles in ethylene glycol. *Nanostruct. Mater.* **1999**, *11*, 1277–1284. [[CrossRef](#)]
32. Quinson, J.; Inaba, M.; Neumann, S.; Swane, A.A.; Bucher, J.; Simonsen, S.B.; Kuhn, L.T.; Kirkensgaard, J.J.K.; Jensen, K.M.O.; Oezaslan, M.; et al. Investigating Particle Size Effects in Catalysis by Applying a Size-Controlled and Surfactant-Free Synthesis of Colloidal Nanoparticles in Alkaline Ethylene Glycol: Case Study of the Oxygen Reduction Reaction on Pt. *ACS Catal.* **2018**, *8*, 6627–6635. [[CrossRef](#)]
33. Neumann, S.; Grotheer, S.; Tielke, J.; Schrader, I.; Quinson, J.; Zana, A.; Oezaslan, M.; Arenz, M.; Kunz, S. Nanoparticles in a box: A concept to isolate, store and re-use colloidal surfactant-free precious metal nanoparticles. *J. Mater. Chem. A* **2017**, *5*, 6140–6145. [[CrossRef](#)]
34. Jerome, F.S.; Tseng, J.T.; Fan, L.T. Viscosities of aqueous glycol solutions. *J. Chem. Eng. Data* **1968**, *13*, 496. [[CrossRef](#)]
35. Quinson, J.; Kunz, S.; Arenz, M. Beyond Active Site Design: A Surfactant-Free Toolbox Approach for Optimized Supported Nanoparticle Catalysts. *ChemCatChem* **2021**, *13*, 1692–1705. [[CrossRef](#)]
36. Nalawade, P.; Mukherjee, T.; Kapoor, S. Green Synthesis of Gold Nanoparticles Using Glycerol as a Reducing Agent. *Adv. Nanopart.* **2013**, *2*, 76–86. [[CrossRef](#)]
37. Inaba, M.; Zana, A.; Quinson, J.; Bizzotto, F.; Dosche, C.; Dworzak, A.; Oezaslan, M.; Simonsen, S.B.; Kuhn, L.T.; Arenz, M. The Oxygen Reduction Reaction on Pt: Why Particle Size and Interparticle Distance Matter. *ACS Catal.* **2021**, *11*, 7144–7153. [[CrossRef](#)]
38. Haiss, W.; Thanh, N.T.K.; Aveyard, J.; Fernig, D.G. Determination of size and concentration of gold nanoparticles from UV-vis spectra. *Anal. Chem.* **2007**, *79*, 4215–4221. [[CrossRef](#)]
39. Hendel, T.; Wuithschick, M.; Kettemann, F.; Birnbaum, A.; Rademann, K.; Polte, J. In Situ Determination of Colloidal Gold Concentrations with UV-vis Spectroscopy: Limitations and Perspectives. *Anal. Chem.* **2014**, *86*, 11115–11124. [[CrossRef](#)]

40. Larm, N.E.; Essner, J.B.; Thon, J.A.; Bhawawet, N.; Adhikari, L.; St Angelo, S.K.; Baker, G.A. Single Laboratory Experiment Integrating the Synthesis, Optical Characterization, and Nanocatalytic Assessment of Gold Nanoparticles. *J. Chem. Educ.* **2020**, *97*, 1454–1459. [[CrossRef](#)]
41. Ye, Y.J.; Lv, M.X.; Zhang, X.Y.; Zhang, Y.X. Colorimetric determination of copper(II) ions using gold nanoparticles as a probe. *RSC Adv.* **2015**, *5*, 102311–102317. [[CrossRef](#)]
42. Agarwal, S.; Mishra, P.; Shivange, G.; Kodipelli, N.; Moros, M.; de la Fuente, J.M.; Anindya, R. Citrate-capped gold nanoparticles for the label-free detection of ubiquitin C-terminal hydrolase-1. *Analyst* **2015**, *140*, 1166–1173. [[CrossRef](#)]
43. Merk, V.; Rehbock, C.; Becker, F.; Hagemann, U.; Nienhaus, H.; Barcikowski, S. In Situ Non-DLVO Stabilization of Surfactant-Free, Plasmonic Gold Nanoparticles: Effect of Hofmeister’s Anions. *Langmuir* **2014**, *30*, 4213–4222. [[CrossRef](#)]
44. Thanh, N.T.K.; Maclean, N.; Mahiddine, S. Mechanisms of Nucleation and Growth of Nanoparticles in Solution. *Chem. Rev.* **2014**, *114*, 7610–7630. [[CrossRef](#)]
45. Siiman, O.; Hsu, W.P. Surface-enhanced Raman-scattering (SERS) enhancements and excitation profiles for 3,5-pyridinedicarboxylate and dabsyl aspartate on colloidal gold. *J. Chem. Soc. Faraday Trans. I* **1986**, *82*, 851–867. [[CrossRef](#)]
46. Quinson, J.; Aalling-Frederiksen, O.; Dacayan, W.L.; Bjerregaard, J.D.; Jensen, K.D.; Jørgensen, M.R.V.; Kantor, I.; Sørensen, D.R.; Theil Kuhn, L.; Johnson, M.S.; et al. Surfactant-free colloidal syntheses of gold-based nanomaterials in alkaline water and mono-alcohol mixtures. *Chem. Mater.* **2023**, *in press*. [[CrossRef](#)]
47. El Amri, N.; Roger, K. Polyvinylpyrrolidone (PVP) impurities drastically impact the outcome of nanoparticle syntheses. *J. Colloid Interface Sci.* **2020**, *576*, 435–443. [[CrossRef](#)] [[PubMed](#)]
48. Quinson, J.; Bucher, J.; Simonsen, S.B.; Kuhn, L.T.; Kunz, S.; Arenz, M. Monovalent Alkali Cations: Simple and Eco-Friendly Stabilizers for Surfactant-Free Precious Metal Nanoparticle Colloids. *ACS Sustain. Chem. Eng.* **2019**, *7*, 13680–13686. [[CrossRef](#)]
49. Strmcnik, D.; Kodama, K.; van der Vliet, D.; Greeley, J.; Stamenkovic, V.R.; Markovic, N.M. The role of non-covalent interactions in electrocatalytic fuel-cell reactions on platinum. *Nat. Chem.* **2009**, *1*, 466–472. [[CrossRef](#)]

Disclaimer/Publisher’s Note: The statements, opinions and data contained in all publications are solely those of the individual author(s) and contributor(s) and not of MDPI and/or the editor(s). MDPI and/or the editor(s) disclaim responsibility for any injury to people or property resulting from any ideas, methods, instructions or products referred to in the content.